Tectonophysics 677–678 (2016) 88–98

Contents lists available at ScienceDirect

Tectonophysics

journal homepage: www.elsevier.com/locate/tecto

Seismic properties of lawsonite eclogites from the southern Motagua fault zone, Guatemala

Daeyeong Kim [a,b,c,*], Simon Wallis [c], Shunsuke Endo [d], Jin-Han Ree [b]

[a] Division of Polar Earth-System Sciences, Korea Polar Research Institute (KOPRI), Incheon, Republic of Korea
[b] Department of Earth and Environmental Sciences, Korea University, Seoul, Republic of Korea
[c] Department of Earth and Planetary Sciences, Nagoya University, Nagoya, Japan
[d] Institute of Geology and Geoinformation, National Institute of Advanced Industrial Science and Technology (AIST), Tsukuba, Japan

ARTICLE INFO

Article history:
Received 2 November 2015
Received in revised form 31 March 2016
Accepted 4 April 2016
Available online 8 April 2016

Keywords:
Electron backscatter diffraction (EBSD)
Crystal preferred orientation (CPO)
Seismic anisotropy
Subducting oceanic crust
Eclogite
Lawsonite

ABSTRACT

We present new data on the crystal preferred orientation (CPO) and seismic properties of omphacite and lawsonite in extremely fresh eclogite from the southern Motagua fault zone, Guatemala, to discuss the seismic anisotropy of subducting oceanic crust. The CPO of omphacite is characterized by (010)[001], and it shows P-wave seismic anisotropies (AV_P) of 1.4%–3.2% and S-wave seismic anisotropies (AV_S) of 1.4%–2.7%. Lawsonite exhibits (001) planes parallel to the foliation and [010] axes parallel to the lineation, and seismic anisotropies of 1.7%–6.6% AV_P and 3.4%–14.7% AV_S. The seismic anisotropy of a rock mass consisting solely of omphacite and lawsonite is 1.2%–4.1% AV_P and 1.8%–6.8% AV_S. For events that propagate more or less parallel to the maximum extension direction, X, the fast S-wave velocity (V_S) polarization is parallel to the Z in the Y–Z section (rotated from the X–Z section), causing trench-normal seismic anisotropy for orthogonal subduction. Based on the high modal abundance and strong fabric of lawsonite, the AV_S of eclogites is estimated as ~11.7% in the case that lawsonite makes up ~75% of the rock mass. On this basis, we suggest that lawsonite in both blueschist and eclogite may play important roles in the formation of complex pattern of seismic anisotropy observed in NE Japan: weak trench-parallel anisotropy in the forearc basin domains and trench-normal anisotropy in the backarc region.

1. Introduction

Lawsonite has attracted attention not only on account of its stability under high-pressure and low-temperature conditions, but also because of its role in the water budget of subducting oceanic crust (Schmidt and Poli, 1994; Ono, 1998; Schmidt and Poli, 1998; Okamoto and Maruyama, 1999; Sinogeikin et al., 2000; Hacker and Abers, 2004; Mainprice and Ildefonse, 2009; van Keken et al., 2011; Reynard and Bass, 2014). The importance of lawsonite under such conditions has become even more prominent on account of recent studies of naturally and experimentally deformed blueschists (Bezacier et al., 2010; Fujimoto et al., 2010; Teyssier et al., 2010; Chantel et al., 2012; Kim et al., 2013a; Cao et al., 2014; Kim et al., 2015). Previous electron backscattered diffraction (EBSD) studies on natural blueschists suggest that lawsonite is a plausible source of the complex patterns of seismic anisotropy in subduction zones (e.g., Kim et al., 2013b). However, published data on lawsonite eclogites are scarce, highlighting the importance of the present study into the seismic properties of lawsonite-bearing eclogite.

Previous studies on the seismic properties of eclogites have reported a weak S-wave splitting of less than ~5%, controlled mainly by omphacite (Ábalos et al., 2011; Worthington et al., 2013). Kim et al. (2013b) proposed a new scheme showing that trench-normal anisotropy in fore-arc basins beneath NE Japan might be attributed to the seismic properties of lawsonite in eclogites. Therefore, here we report on the seismic properties of extremely fresh lawsonite eclogites from the southern Motagua fault zone (MFZ), Guatemala, as assessed mainly by EBSD analyses. In addition, we discuss the tectonic implications of seismic anisotropy caused by lawsonite eclogites in subduction zones.

2. Geological outline

The MFZ is a sinistral suture at the boundary of the North American plate (Maya block) and the Caribbean plate (Chortís block), located in Guatemala (Dengo, 1985; Beccaluva et al., 1995). Eclogite and jadeite occur commonly as tectonic blocks within antigorite serpentinite mélange (the El Tambor complex) (Fig. 1). The northern MFZ (NMFZ) mélange has been thrust northward over the Chuacús complex, while the southern MFZ (SMFZ) mélange, comprising pristine lawsonite eclogites and blueschists (Harlow et al., 2004; Tsujimori et al., 2005, 2006), has been thrust southward over the very low-grade San Diego phyllites of the Chortís basement rocks (Marroni et al., 2009; Ratschbacher et al., 2009). The similar Sm–Nd isochron ages (~132 Ma; Brueckner et al., 2009) of eclogite blocks from both the NMFZ and SMFZ mélanges, combined with different $^{40}Ar/^{39}Ar$ phengite ages (77–65 Ma for the NMFZ rocks and 125–116 Ma for the SMFZ

* Corresponding author.
E-mail address: dkim@kopri.re.kr (D. Kim).

http://dx.doi.org/10.1016/j.tecto.2016.04.012
0040-1951/

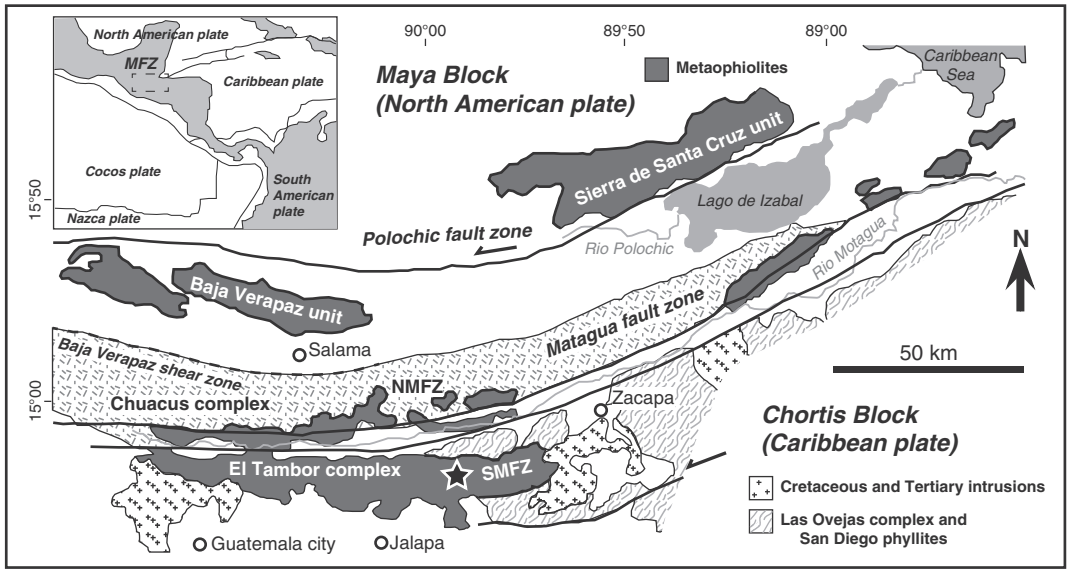

Fig. 1. Simplified geological map of the Motagua fault zone (MFZ), Guatemala (modified from Marroni et al., 2009). The analyzed samples, which show very good preservation of mineralogy and microstructures formed near the peak of burial, were collected from the southern Motagua fault zone (SMFZ).

rocks; Harlow et al., 2004), suggest comparable eclogite-facies metamorphism in both mélanges, but with differing retrograde histories. The tectonic relationship of the two mélanges remains debated (e.g., Brueckner et al., 2009; Ortega-Gutiérrez et al., 2007). The peak metamorphic *P–T* conditions of the SMFZ lawsonite eclogites have been estimated as ~26 kbar and ~480 °C by Tsujimori et al. (2006), and as ~25 kbar and ~520 °C by Endo et al. (2012).

3. Analytical techniques

The crystallographic preferred orientations (CPOs) of the main rock-forming minerals in the eclogite (i.e., omphacite and lawsonite) were measured by indexing EBSD patterns (Randle, 1992; Prior et al., 1999; Randle and Engler, 2000) using an Oxford–HKL EBSD on a JEOL JSM-6510LV scanning electron microscope (SEM) at Nagoya University, Japan. The CPO measurements were performed using an accelerating voltage of 20 kV, a working distance of 27 mm, and a beam current of ~10 nA. We used a low vacuum mode (~10 Pa), and therefore the samples were not coated. Automatic mapping of each sample (1-μm step size) was performed to examine the influence on lattice orientations of compositional zoning in omphacite and lawsonite. After confirming that the lattice orientation was independent of compositional variations, the EBSD patterns were manually indexed by examining single points within each grain. The population of grains was standardized at ~250 to ensure the reliability of data and to allow for comparisons among samples. Pole figures were plotted using the software PFch5 (written by D. Mainprice), and fabric strength is expressed using the *J*-index (Bunge, 1982; Mainprice and Silver, 1993).

The seismic properties of omphacite, lawsonite, and whole-rock masses consisting of omphacite and lawsonite were calculated so as to understand the influence of minerals on seismic properties in subduction zones. The P-wave seismic anisotropy (AV_P) is generally defined as the difference between the maximum and minimum velocities along two dissimilar propagation paths, expressed as a percentage; e.g., $200(V_{Pmax} - V_{Pmin}) / (V_{Pmax} + V_{Pmin})$. The S-wave seismic anisotropy (AV_S) is generally defined as the percentage difference between dissimilar velocities of two orthogonally polarized S-waves individually propagating through an anisotropic medium; in this study, AV_S was evaluated as $200(V_{S1} - V_{S2}) / (V_{S1} + V_{S2})$, where V_{S1} and V_{S2} are the fast and slow velocities, respectively.

The seismic properties of a rock mass were calculated with reference to the modal abundances of each mineral (Mainprice, 1990; Mainprice et al., 2000) (Table 1). We employed the respective single crystal elastic constants (C_{ij}) of omphacite (Bhagat et al., 1992) and lawsonite (Sinogeikin et al., 2000), and their densities using the Voigt–Reuss–Hill averaging scheme.

4. Microstructures of SMFZ eclogites

The specimens from the SMFZ are fine-grained eclogites consisting mainly of omphacite, lawsonite, garnet, and phengite. The retrogressed (sample GM5) and very fresh (samples GM9, GM17, GM13, and GM18) hydrous eclogites were selected on account of their high lawsonite and omphacite contents. Different microstructures, governed mainly by the omphacite content, occur in the matrix of each sample. Sample GM5 shows large relict garnet crystals and large idioblastic grains of lawsonite, glaucophane, phengite, rutile, and omphacite as the main constituents of the matrix (Fig. 2a). Glaucophane and patches of lawsonite and phengite in the matrix are the products of retrograde lawsonite blueschist-facies overprinting (Endo et al., 2012). Sample GM9 contains large grains of omphacite, acicular lawsonite, and

Table 1
Sample locations and the results of fabric analysis.

Sample numbers	Lithology*	Mode** (%)	Minerals	Fabric strength (CPO)		Seismic anisotropy (%)	
				N	J	AV_P	AV_S
GM5	Highly retrogressed eclogite	Omp23, Grt19, Lws19, Gln19, Ph7, Chl7	Omp	250	5.3	1.4	1.56
			Lws	250	3.7	5.1	9.61
GM9	Metadolerite	Omp47, Lws22, Grt17, Ph6	Omp	251	8.2	3.2	1.4
			Lws	249	4.7	4.9	9.0
GM17	Metabasalt (Hydrous eclogite)	Omp38, Lws22, Grt20, Ph12	Omp	250	5.6	1.6	1.43
			Lws	250	2.9	1.7	3.38
GM13	Metabasalt (Hydrous eclogite)	Omp48, Lws27, Grt15, Chl5	Omp	250	11.5	2.7	2.65
			Lws	250	4.7	6.6	14.71
GM18	Metabasalt (Hydrous eclogite)	Omp43, Lws28, Grt15, Ph9	Omp	250	9.6	2.8	2.06
			Lws	250	4.1	6.3	12.90

We follow the terms of lithology* in Endo et al. (2012). Mode** excludes titanite, and quartz (abundances of each mineral are less than 5%). Chl: chlorite; Gln: glaucophane; Grt: garnet; Lws: lawsonite; Omp: omphacite; Ph: phengite; N: number of measurements; J: *J*-index.

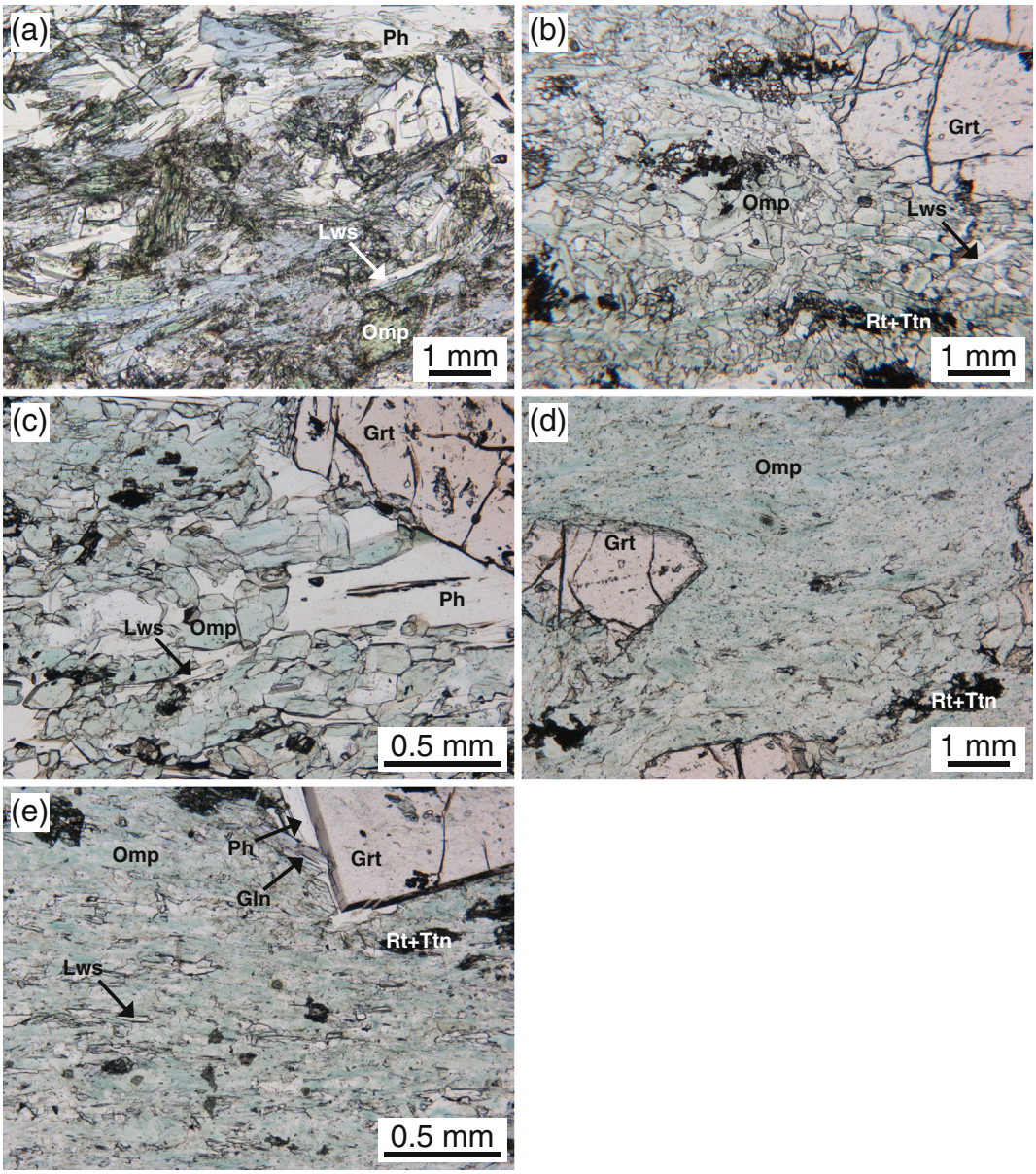

Fig. 2. Photomicrographs of analyzed samples (XZ sections, the lineation is horizontal in the images) taken under plane polarized light. Samples were subdivided into highly retrogressed eclogite (a: sample GM5), metadolerite (b: sample GM9), and hydrous eclogites (c: sample GM17; d: sample GM13; e: sample GM18). Mineral abbreviations and rock classifications are after Whitney and Evans (2010) and Endo et al. (2012), respectively. Gln: glaucophane; Grt: garnet; Lws: lawsonite; Omp: omphacite; Ph: phengite; Rt: rutile; Ttn: titanite.

relatively abundant rutile and titanite in the matrix (Fig. 2b). The garnet contains numerous inclusions of lawsonite, omphacite, rutile, titanite, and pyrrhotite. Because a relic igneous fabric (porphyritic texture) is present in sample GM9, it was subdivided into metadolerite (Endo et al., 2012). Sample GM17 is composed of omphacite (38 vol.%), lawsonite (22 vol.%), garnet (20 vol.%), and relatively large amounts of phengite (12 vol.%) (Fig. 2c). Samples GM13 and GM18 represent the most common type of eclogite (metabasalt) in the SMFZ; these samples typically contain subhedral lawsonite with very fine-grained acicular omphacite in the matrix (Fig. 2d and f), and both samples contain relatively low abundances of garnet and abundant omphacite and lawsonite. The garnet commonly contains sigmoidal inclusion trails that are continuous with the matrix schistosity, and the results of phase equilibria modeling suggest that the garnet grew under conditions of increasing pressure and temperature (Endo et al., 2012). Such conditions indicate that the shape preferred orientations of omphacite and lawsonite in the matrix formed contemporaneously with subduction-stage ductile deformation, although minor retrograde (post-kinematic) generations of the two minerals are also recognized. In this study, omphacite and lawsonite in the matrix of the analyzed samples were the main targets of analysis.

5. Results

Pole figures of omphacite in the SMFZ eclogites typically display (010) planes subparallel to the foliation and [001] axes subparallel to the lineation (Fig. 3), which is consistent with the results of previous studies (Bascou et al., 2001, 2002; Zhang and Green, 2007). The value of the *J*-index is low for highly retrogressed eclogite (5.3 for sample GM5) but high for fresh hydrous eclogite (e.g. 11.5 for sample GM13) (Table 1). The CPOs of lawsonite in blueschists and eclogites show [100] or [010] maxima subparallel to the lineation and [001] maxima subnormal to the lineation (Fig. 3b, d, f, h, and j) (Kim et al., 2013a; Cao et al., 2014). The *J*-index values for lawsonite are in the range of 2.9 (sample GM17) to 4.7 (samples GM9 and GM13). Therefore, omphacite in the matrix has a stronger CPO than does lawsonite.

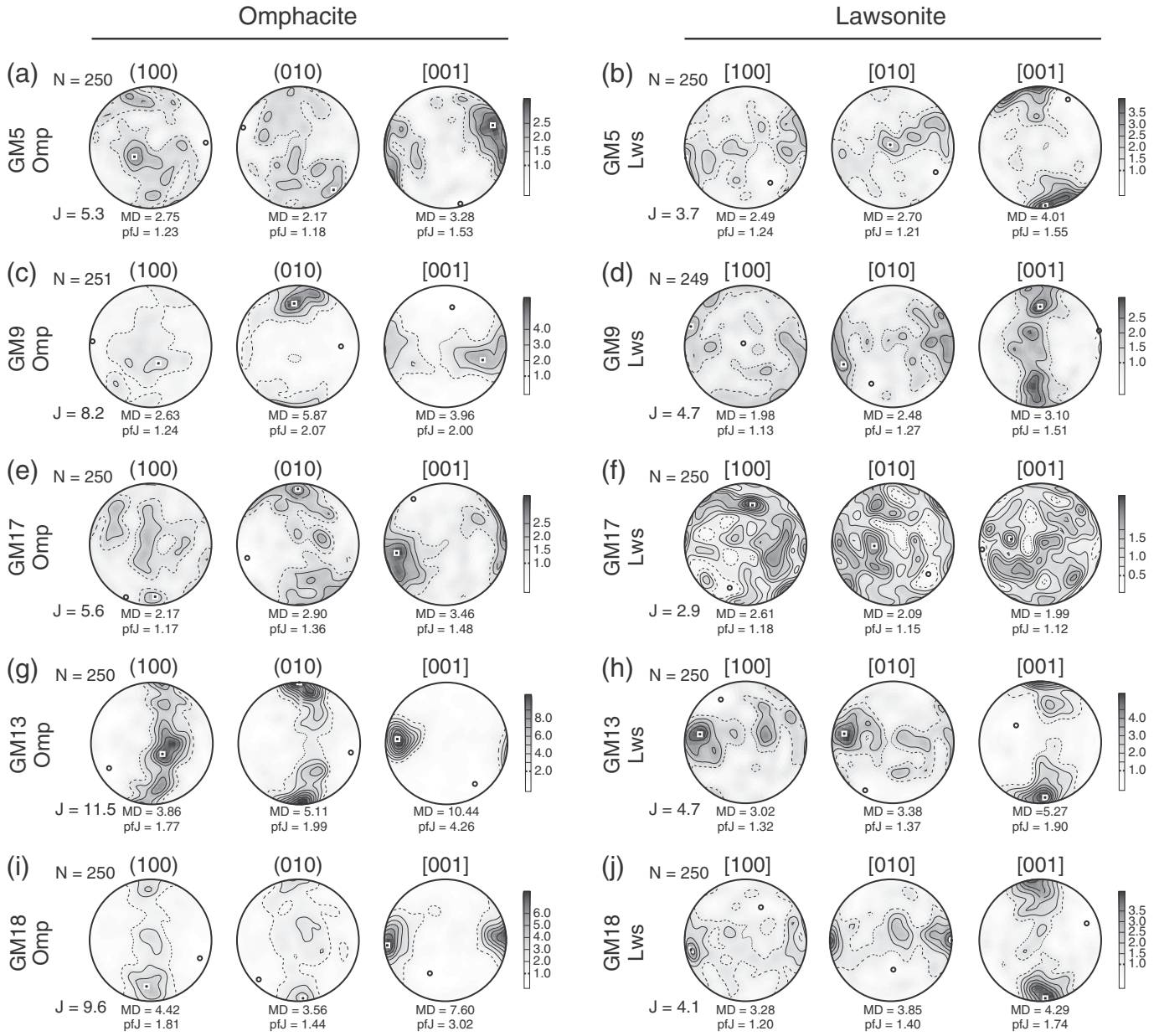

Fig. 3. Crystal preferred orientations (CPOs) of omphacite and lawsonite in the analyzed samples. Poles are plotted on a lower-hemisphere equal-area projection and contours are in multiples of uniform distribution (m.u.d). N: Number of measurements; J: *J*-index; MD: maximum density; pfJ: pole figure *J*-index.

The V_P, AV_S, and V_{S1} polarizations of omphacite, lawsonite, and whole rock for the SMFZ eclogites (and their rotated polarizations; V_{S1} is rotated in the figures) are calculated and plotted on a lower hemisphere projection in Figs. 4, 5, and 6, respectively. The seismic properties of omphacite are estimated as V_P = 8.29–8.56 km/s, with seismic anisotropies of AV_P = 1.4%–3.2% and AV_S = 1.35%–2.65% (Fig. 4). Relatively strong anisotropies in the hydrous eclogites (of $AV_S > 2\%$; samples GM13 and GM18) show a maximum V_P direction subnormal to the lineation and foliation. AV_S and V_{S1} polarization directions show complex changes with orientation. Lawsonite shows an estimated V_P value of 7.71–8.27 km/s and strong seismic anisotropies of AV_P = 1.7%–6.6% and AV_S = 3.4%–14.7% (Fig. 5). The maximum V_P of lawsonite is usually perpendicular to the foliation. High AV_S values generally form a girdle distribution sub perpendicular to the foliation with a concentration parallel to the Y direction and V_{S1} polarization direction lies parallel to the Z direction.

The seismic properties of rock masses are generally evaluated under the assumption that the rock is composed only of limited number of minerals (e.g., Morales and Tommasi, 2011). In this study, we assumed that omphacite and lawsonite are the main constituents of lawsonite eclogites, and the calculated seismic properties of rock masses are based on the summed characteristics of those of omphacite and lawsonite. The V_P of lawsonite eclogites was evaluated as 8.03–8.37 km/s, with anisotropies of AV_P = 1.2–4.1% and AV_S = 1.8–6.8% (Fig. 6). The V_{S1} polarization is developed subnormal to the foliation.

6. Discussion

6.1. Seismic properties of lawsonite eclogite

Seismic properties of rocks can be computed using crystallographic orientation data. Therefore, the pole figures of minerals in lawsonite eclogites present in this study can be used to facilitate an understanding of the geologic implications of seismic anisotropy observed in modern subduction zones where similar rock types are thought to be forming

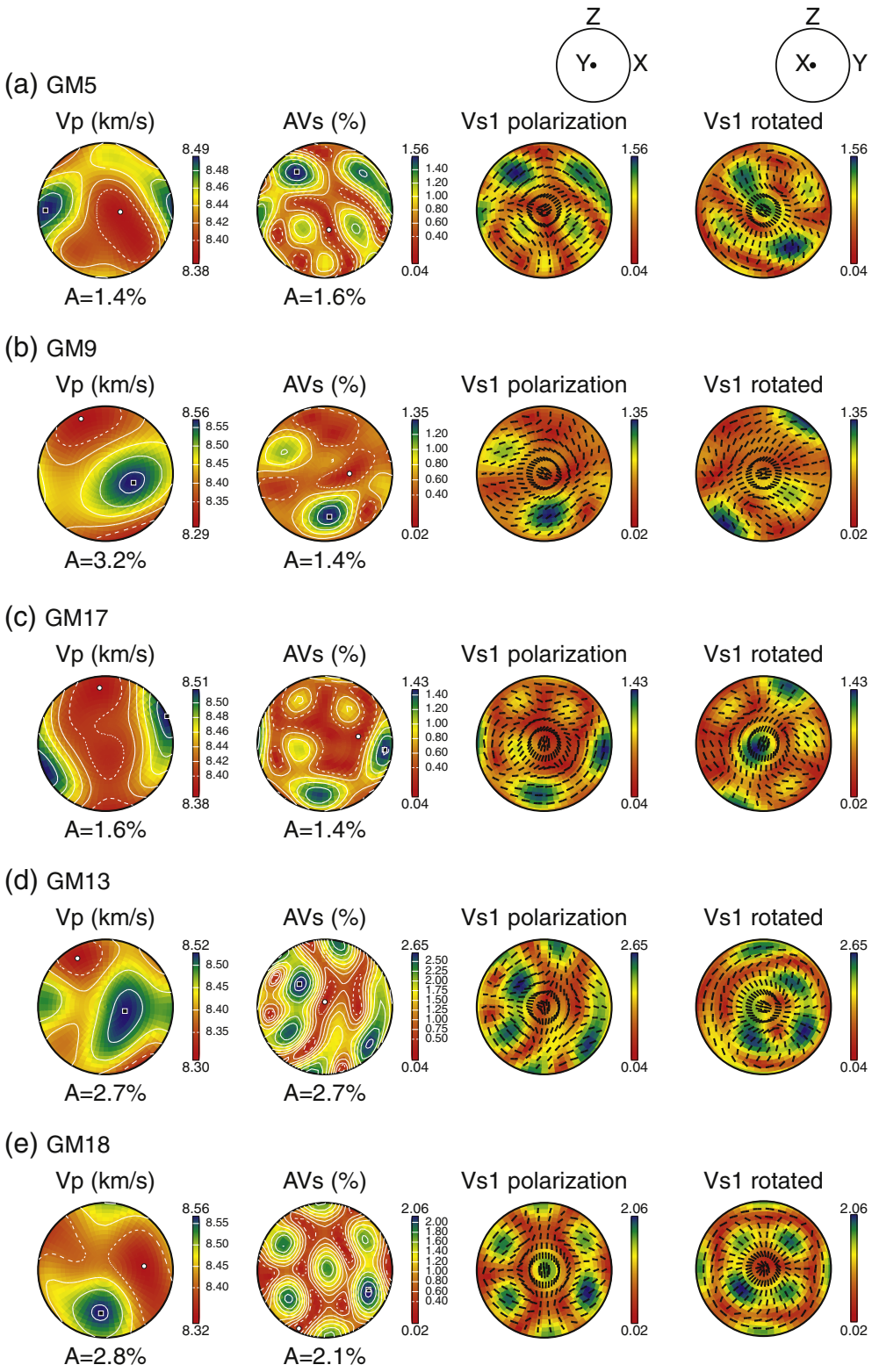

Fig. 4. Calculated seismic properties of omphacite. Polarization and rotation of V_S1 are shown in the XZ and YZ sections, respectively. The Voigt–Reuss–Hill averaging scheme was used and data are plotted in equal-area lower-hemisphere projections. V_P: P-wave velocity; AV_S: S-wave anisotropy; A: anisotropy.

at depth. The CPOs of omphacite and lawsonite in the SMFZ eclogites in this study are similar to those of omphacite reported in lawsonite-free eclogites (Bascou et al., 2001, 2002; Zhang and Green, 2007) and lawsonite in blueschists (Kim et al., 2013a, Cao et al., 2014). In sample GM9, the mean density of (010) for omphacite is slightly higher than that of [001], and lawsonite shows a girdle-type CPO (at relatively low abundances of lawsonite); the seismic anisotropy of lawsonite is, therefore, relatively low (Figs. 3 and 6; Table 1). Lawsonite in sample GM17 is scarce and shows a weak CPO. Consequently, the seismic anisotropy is weak (Figs. 3 and 6; Table 1) and the abundance of lawsonite and its CPO are the predominant controls on the seismic properties of the rock mass.

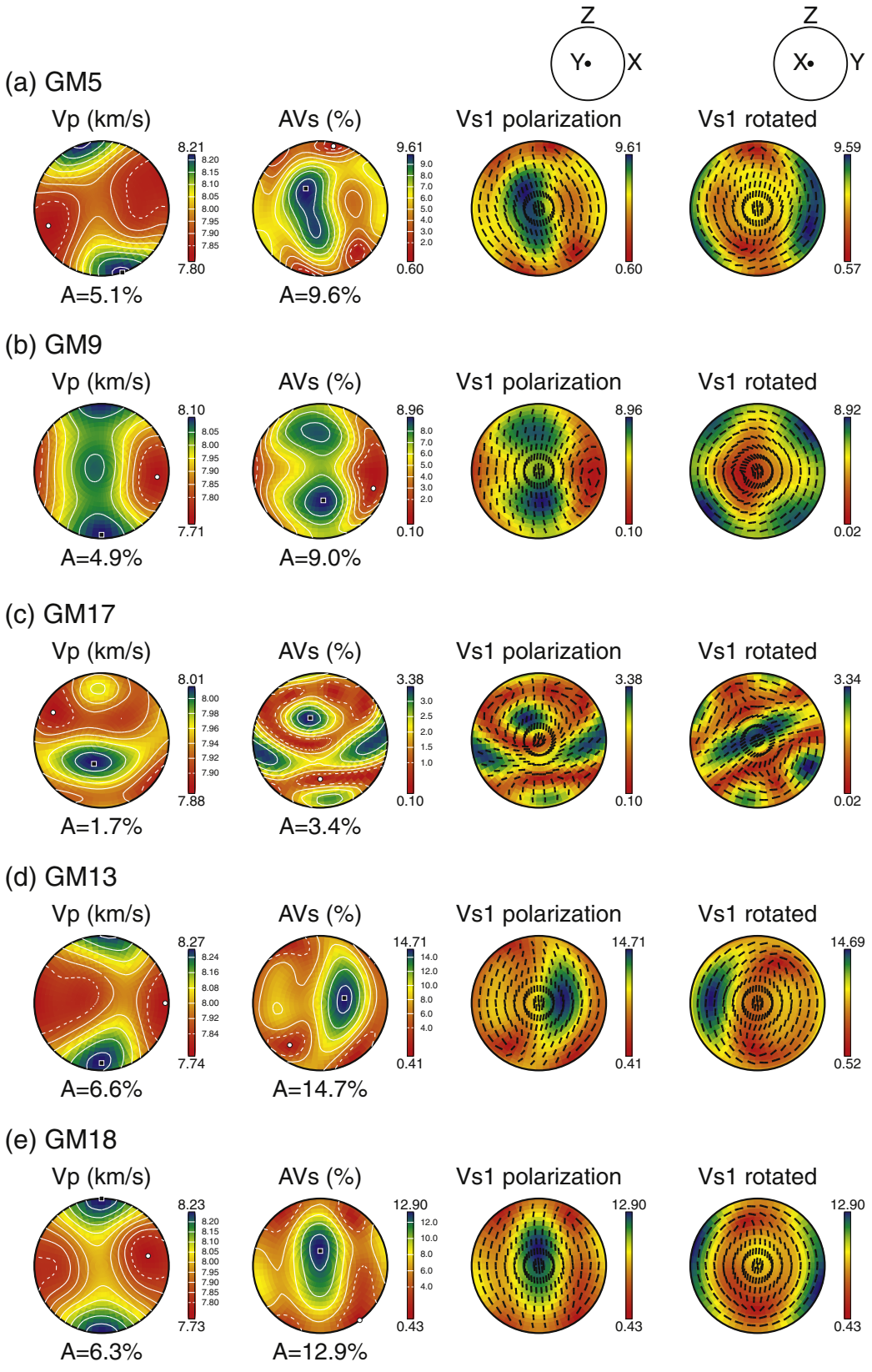

Fig. 5. Estimated seismic properties of lawsonite. Polarization and rotated view of V_S1 values showing the development of maximum values subnormal to the foliation and lineation, indicating the occurrence of trench-normal fast anisotropy. Symbols are as in Fig. 4.

The lawsonite eclogite samples examined in this study show very good preservation of mineralogy and microstructures formed near the peak of burial. However, high-grade metamorphic rocks commonly undergo strong deformation and metamorphism during exhumation and the observed mineralogy and microstructure may not be representative of the condition at peak depth. These factors have to be taken into

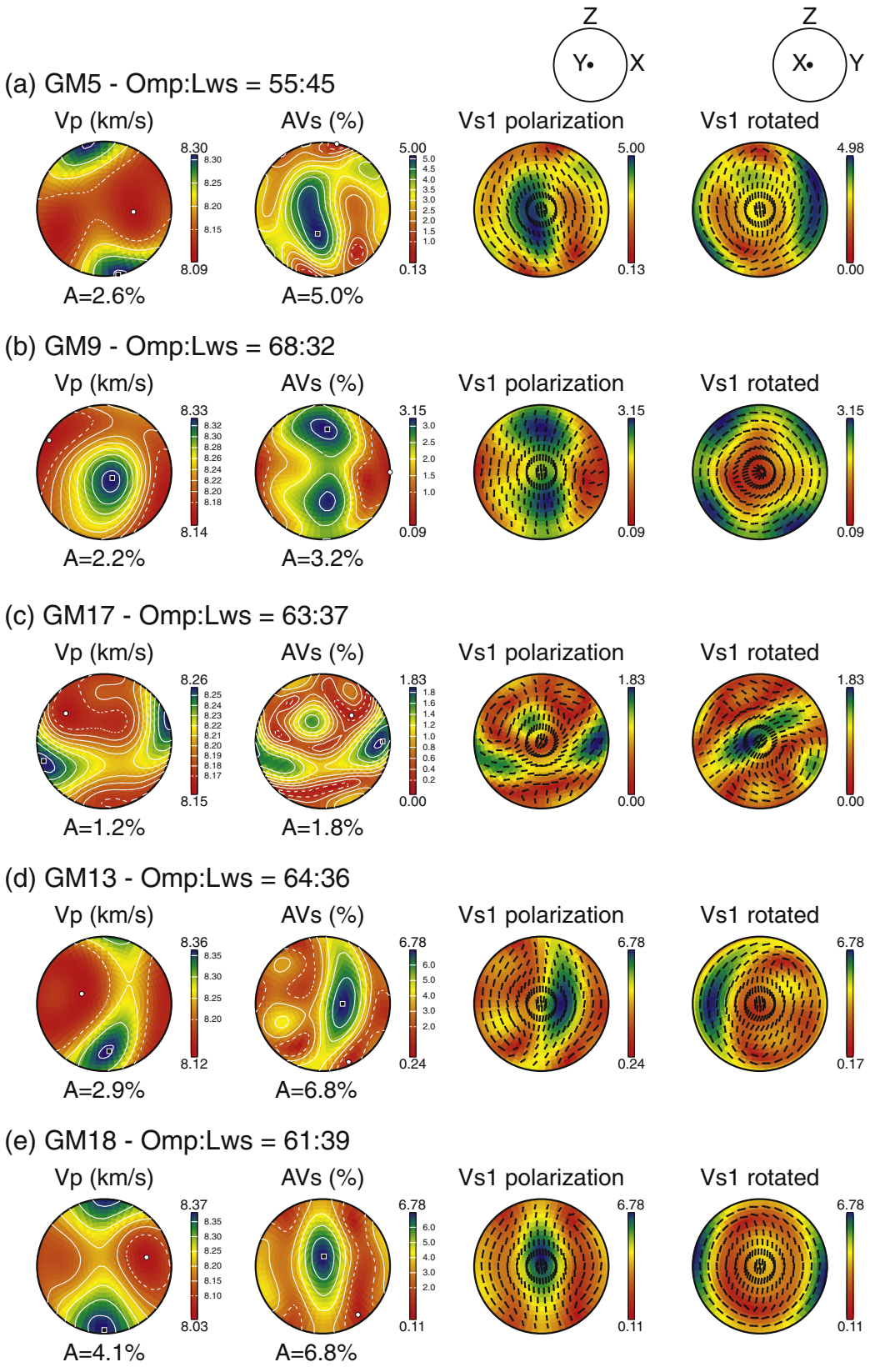

Fig. 6. Seismic anisotropy evaluated for each lawsonite eclogite sample; the samples are assumed to be composed only of omphacite and lawsonite. Similar polarization and rotation of V_S1 to that shown in Fig. 5 suggesting the occurrence of trench-normal fast anisotropy caused by lawsonite eclogite and emphasizing the dominant role of lawsonite. Symbols are as in Fig. 4.

consideration when comparing our results with other studies of natural examples. It is also important to compare the results from studies of natural samples with experimental data where the conditions of deformation are tightly constrained. The V_P of SMFZ eclogites calculated based solely on the CPO and proportions of lawsonite and omphacite gives a range of 8.03–8.37 km/s. This range is very similar to those

derived in previous studies of natural and experimental material (8.3–8.4 km/s by Fountain et al., 1994; ~8 km/s by Christensen and Mooney, 1995; 7.42–7.82 km/s by Kern et al., 1999; 8.6 km/s by Bascou et al., 2001; 8.68–8.80 km/s by Zhang and Green, 2007; 7.26–8.39 km/s by Ábalos et al., 2011; 7.92–8.28 km/s by Cao et al., 2013) and supports the approach taken here to estimate bulk rock properties.

6.2. Shear wave polarization occurred by lawsonite eclogite

Shear wave polarization can provide information on the components and structures of the deep Earth (e.g., Katayama et al., 2009). The extremely fresh lawsonite eclogites from the SMFZ in Guatemala exhibit a relatively strong seismic anisotropy. This suggests that lawsonite may play an important role in the development of seismic anisotropy in subduction zones and closer study of this issue is important. The SMFZ eclogites exhibit a V_S1 polarization subnormal to the foliation (Fig. 6). We suggest an assumption that the subduction of oceanic crust generates a simple shear with a shearing direction subparallel to the subduction direction. Hence, the foliation and lineation in subducting oceanic crust are formed parallel to the subduction plane and to the subduction direction, respectively (e.g., Buttles and Olson, 1998; Healy et al., 2009; Kim et al., 2013b). The fast V_S1 polarization of lawsonite eclogites develops subnormal to the subducting direction and associated shear plane, and hence it can produce trench-normal fast anisotropy (Fig. 6). Similar AV_S values shown for lawsonite on its own and combinations of omphacite and lawsonite suggest lawsonite CPO is the dominant cause of seismic anisotropy in such eclogite samples (Figs. 5 and 6). The weakest anisotropies are shown by samples GM9 and GM17. The sample GM17 shows a weak overall lawsonite CPO (Fig. 3f) and is associated with a low J value. Despite its relatively weak anisotropy, GM9 shows a J value comparable with the other samples (Fig. 3c and d). The main difference with other samples is a spread of [001] orientations in a girdle. This suggests that the development of a point concentration of [001] is an important feature in development of seismic anisotropy in these samples. In contrast to the lawsonite eclogite samples examined in this study, seismic properties of epidote eclogites show fast S-wave polarization parallel to the foliation (e.g., Cao et al., 2013), which will result in representing trench-parallel anisotropy for local slab events.

Studies of high P/T metamorphic rocks are an important source of information about the conditions close to the subduction boundary where they form. However, in many cases these rocks undergo deformation during their exhumation (e.g., Ji et al., 2003). Where the metamorphic rocks are found as blocks within a weaker matrix, such as the eclogites used for this study, the blocks remain relatively undeformed during exhumation and are likely to preserve petrofabrics formed deep in the subduction zone. Microstructural and petrological studies show the mineral fabrics of the lawsonite eclogite samples examined in this study were formed close to peak conditions and there has been little retrogression or post-peak P ductile deformation. Hence, the fresh eclogites of this study can be used to discuss the relationship between fabrics of metamorphic rocks and patterns of seismic anisotropy observed in present day convergent margins.

6.3. Applications of seismic properties of lawsonite eclogite to nature

The seismic anisotropy of epidote eclogite is generally relatively weak due to the weak seismic anisotropy of omphacite and the lack of lawsonite (e.g., Bezacier et al., 2010). The AV_S generated in lawsonite eclogites in the SMFZ (1.8%–6.8%) are relatively strong compared with results reported for other natural eclogites (Worthington et al., 2013). These differences are likely related to the modal abundance, freshness, and fabric strength of samples; consequently, we consider each of these factors in turn.

Thermal modeling suggests large parts of subducted oceanic crust will experience cooler thermal gradients than those shown by most known metamorphic rocks. Despite the lack of examples in the rock record, thermodynamic modeling can be used to predict the nature of such very cold eclogitic rocks. Endo et al. (2012) uses this approach to show that very cold eclogite would contain a large proportion of hydrous phases including lawsonite. In the present study, calculations of seismic anisotropy with different modal abundances show values of V_P = 7.97–8.34 km/s, V_S = 4.18–4.62 km/s, and AV_S = 2.18%–8.21% (Fig. 7). Small reductions in AV_S in lawsonite-poor areas are due to the counteracting effects of omphacite (e.g., Kim et al., 2013b). High modal abundances of lawsonite observed in other studies (generally up to 40 modal % (Davis and Whitney, 2006), occasionally up to 50 vol.% (Okay, 1980), and rarely up to ~75 vol.% (Vitale Brovarone and Beyssac, 2014)) confirm the general importance of this mineral in controlling the seismic properties. A rock consisting of 75% lawsonite and 25% omphacite is expected to show AV_S of around 11.7% (Fig. 7).

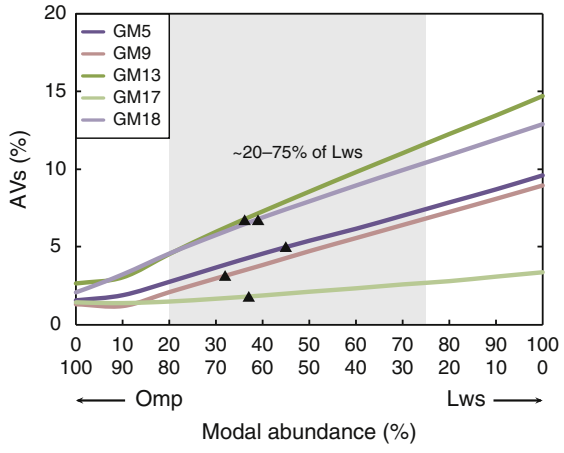

Fig. 7. AV_S versus modal abundance for samples of the present study. The AV_S values of eclogites were computed from the seismic anisotropies of omphacite and lawsonite at 10% increments. The small decrease shown by a rock consisting of 90% omphacite and 10% lawsonite is attributed to the dominant effect of omphacite. Triangles indicate modal abundance of each sample in this study.

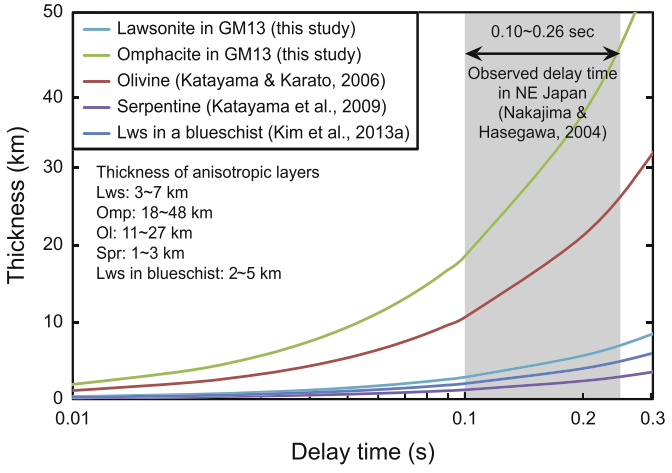

Fig. 8. Relationship between the thickness of an anisotropic layer and delay time. An anisotropic layer of lawsonite with a thickness of 3–7 km is needed to explain the observed delay time beneath NE Japan (0.10–0.26 s; Nakajima and Hasegawa, 2004). For comparison, the figure also slows the thicknesses of an anisotropic layer of olivine (AV_S = 4.5%, $<V_S>$ = 4.75 km/s; Katayama and Karato, 2006), serpentine (AV_S = 35.9%, $<V_S>$ = 4.13 km/s; Katayama et al., 2009), and lawsonite in blueschist (AV_S = 21.3%, $<V_S>$ = 4.15 km/s; Kim et al., 2013a).

The fabric strength of minerals is also an important control on the seismic properties of SMFZ eclogites. Previous studies on lawsonite blueschists have found that the fabric strength of lawsonite is strong ($J = 7.8–9.6$, Kim et al., 2013a) relative to the values for eclogite determined in this study ($J = 2.9–4.7$). This discrepancy is probably related to different degrees of deformation during exhumation or strength contrasts between glaucophane and lawsonite in blueschist, and omphacite and lawsonite in eclogite. Irrespective of the mineralogy, large strains are expected to be generated in subducting oceanic crust (Bevis, 1988) due to the shear stresses induced by the contact with mantle, the very small thickness of the subducting slab (~7 ± 1 km; White et al., 1992) and the very large displacements. The transition from blueschist to eclogite in a subduction environment occurs associated with continuous deformation and any lawsonite fabric developed in blueschist is likely to be and transform to eclogite. Shear wave anisotropy of around 20% has been reported in lawsonite blueschist (Kim et al., 2013a). Together with the likelihood of lawsonite-rich eclogite being more common in the subducted ocean crust than reflected in documented examples (e.g., Endo et al., 2012), this indicates that the influence on seismic anisotropy of lawsonite fabrics in the subducting oceanic crust identified in the present study is a minimum estimate.

The thickness of an anisotropic layer is often used in comparisons of seismically anisotropic minerals (e.g., Satsukawa et al., 2011). We compared our data with the seismic properties of other minerals, such as olivine, serpentine, and lawsonite, in a natural blueschist. The thickness (D) is defined by

$$D = <Vs>/AV_S dt,$$

where <Vs> is the average of the fast and slow velocities, AV_S is the anisotropy in a specific propagation direction, and dt is the delay time. Based on the observed delay time in NE Japan (0.1–0.26 s for trench-normal S-wave splitting; Nakajima and Hasegawa, 2004), the thickness

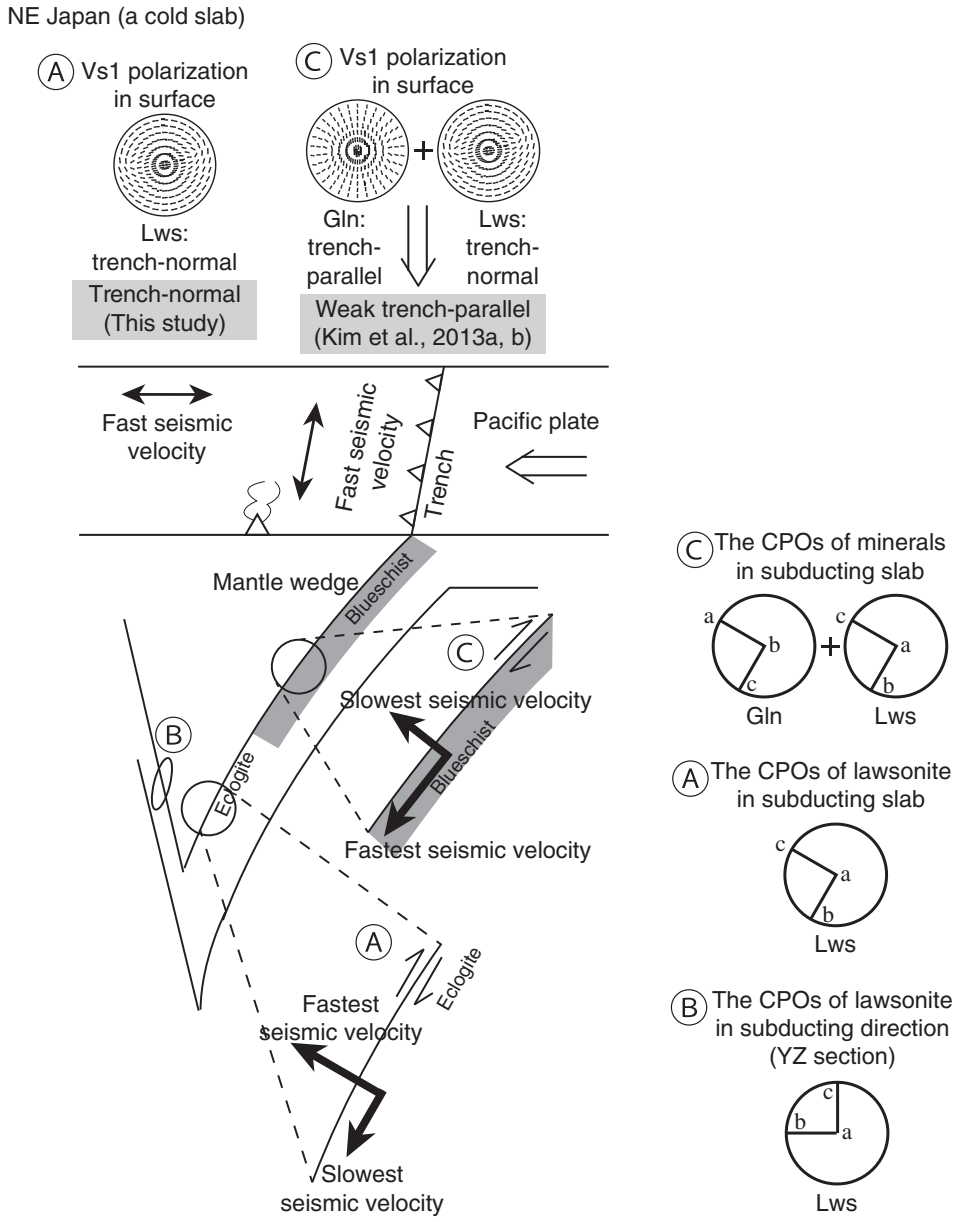

Fig. 9. Schematic model showing trench-parallel fast anisotropy in a forearc basin and trench-normal anisotropy in a backarc basin (modified from Kim et al., 2013b). Seismic properties caused by lawsonite in eclogite (A: in XZ section; B: in YZ section) and glaucophane and lawsonite in blueschist (C, Kim et al., 2013a, 2013b). The patterns of S-wave polarization at the surface are based on a subduction angle of 90°. Gln: glaucophane; Lws: lawsonite.

of the anisotropic layer is calculated as 3–7 km for the lawsonite in sample GM13 (Fig. 8). The thickness of the anisotropic layer is ~18–48 km for omphacite in sample GM13 (however, omphacite generates trench-parallel anisotropy), ~1–3 km for serpentine (Katayama et al., 2009), ~11–27 km for olivine (Katayama and Karato, 2006), and ~2–5 km for lawsonite in blueschist (Kim et al., 2013a). Assuming oceanic crust with a thickness of ~7 ± 1 km (White et al., 1992), the presence of lawsonite in eclogite can explain the trench-normal seismic anisotropy observed in the backarc of NE Japan. Assuming that strong lawsonite fabrics in blueschist can be maintained during the transition from blueschist to eclogite, a small thinner anisotropic layer (~2–5 km) of lawsonite in eclogite satisfies to explain a trench-normal anisotropy beneath NE Japan. In addition, the possible existence of a high modal abundance of lawsonite should be considered in assessing the influence of lawsonite on the development of complex seismic anisotropic patterns in NE Japan. Therefore, the present results suggest that the presence of lawsonite is important in explaining trench-normal seismic anisotropy, and other phases in eclogite (e.g., omphacite and phengite) and the arrangements of olivine in the mantle may also contribute to seismic anisotropy in subduction zones (e.g., Katayama and Karato, 2006; Faccenda et al., 2008; Faccenda and Capitanio, 2013; Precigout and Almqvist, 2014; Cao et al., 2015).

Kim et al. (2013b) argued that complex seismic anisotropic patterns in NE Japan can be explained by the transition from blueschist to eclogite. However, their proposal was not well constrained on account of a lack of anisotropy data from lawsonite eclogites; hence, we first describe our results calculated using extremely fresh SMFZ eclogites. Our tectonic model (Fig. 9) shows that glaucophane in lawsonite blueschists generates relatively weak trench-parallel seismic anisotropy in the forearc basin, and that lawsonite in eclogites produces trench-normal anisotropy in the backarc basin. The transition from blueschist to eclogite is due to the presence of strongly anisotropic minerals, such as glaucophane in blueschist and lawsonite in eclogite. Although blueschist contains lawsonite, which has a stronger seismic crystalline anisotropy than does glaucophane, glaucophane has a stronger fabric because it is mechanically weak (e.g., Kim et al., 2015). Omphacite in eclogites displays a strong CPO, but this CPO may have a weak effect on seismic anisotropy because of the weak anisotropic properties of omphacite. Therefore, our model suggests that lawsonite plays a crucial role in the generation of complex anisotropic patterns in NE Japan; however, additional EBSD analyses of lawsonite eclogites in other places and calculations on seismic properties should be performed to fully understand seismic anisotropy in subduction zones.

7. Conclusions

Using EBSD measurements, we calculated the seismic anisotropy of five lawsonite eclogites from the SMFZ, Guatemala. The trench-normal seismic anisotropy in lawsonite eclogite ranges from 3.4% to 14.7%. Based on the possibility that the modal abundances of lawsonite in the present study are higher than those than observed in previous studies, the lawsonite eclogites of the present study might possess S-wave anisotropies of >11.7% in an anisotropic layer 3–8 km thick. Although the influence of other phases in eclogite, or olivine in the mantle, should be considered, this study suggests that lawsonite plays an important role in the generation of trench-normal anisotropy in subduction zones.

Acknowledgments

The authors appreciate the technical support of T. Nagaya in performing the EBSD analyses. Special thanks to Dr. Bjarne Almqvist and an anonymous reviewer for constructive comments that greatly develop our manuscript. This research was largely funded by a grant from the Japan Society for the Promotion of Science (JSPS) to SW (24244079), with partial funding by grants from the National Research Foundation (NRF) of Korea (NRF-2014R1A1A2056836) and KOPRI projects (PM15030 and PE16050).

References

Ábalos, B., Fountain, D.M., Gil Ibarguchi, J.I., Puelles, P., 2011. Eclogite as a seismic marker in subduction channels: seismic velocities, anisotropy, and petrofabric of Cabo Ortegal eclogite tectonites (Spain). Geol. Soc. Am. Bull. 123, 439–456. http://dx.doi.org/10.1130/B30226.1.

Bascou, J., Barruola, G., Vaucheza, A., Mainprice, D., Egydio-Silva, M., 2001. EBSD-measured lattice-preferred orientations and seismic properties of eclogites. Tectonophysics 342, 61–80. http://dx.doi.org/10.1016/S0040-1951(01)00156-1.

Bascou, J., Tommasi, A., Mainprice, D., 2002. Plastic deformation and development of clinopyroxene lattice preferred orientations in eclogites. J. Struct. Geol. 24, 1357–1368. http://dx.doi.org/10.1016/S0191-8141(01)00137-7.

Beccaluva, L., Bellia, S., Coltorti, M., et al., 1995. The north western border of the Caribbean plate in Guatemala: new geological and petrological data on the Motagua ophiolitic belt. Ofioliti 20, 1–15.

Bevis, M., 1988. Seismic slip and down-dip strain rates in Wadati–Benioff zones. Science 240, 1317–1319. http://dx.doi.org/10.1126/science.240.4857.1317.

Bezacier, L., Reynard, B., Bass, J.D., Wang, J., Mainprice, D., 2010. Elasticity of glaucophane, seismic velocities and anisotropy of the subducted oceanic crust. Tectonophysics 494, 201–210. http://dx.doi.org/10.1016/j.tecto.2010.09.011.

Bhagat, S.S., Bass, J.D., Smyth, J.R., 1992. Single-crystal elastic properties of omphacite-C2/c by brillouin spectroscopy. J. Geophys. Res. 97, 6843–6848. http://dx.doi.org/10.1029/92JB0030.

Brueckner, H.K., Avé Lallemant, H.G., Sisson, V.B., Harlow, G.E., Hemming, S.R., Martens, U., Tsujimori, T., Sorensen, S.S., 2009. Metamorphic reworking of a high pressure-low temperature mélange belt along the Motagua fault, Guatemala: a record of Neocomian and Maastrichtian transpressional tectonics. Earth Planet. Sci. Lett. 284, 228–235. http://dx.doi.org/10.1016/j.epsl.2009.04.032.

Bunge, H.J., 1982. Texture Analysis in Materials Science. Butterworth, London, p. 559.

Buttles, J., Olson, P., 1998. A laboratory model of subduction zone anisotropy. Earth Planet. Sci. Lett. 164, 245–262. http://dx.doi.org/10.1016/S0012-821X(98)00211-8.

Cao, Y., Jung, H., Song, S., 2013. Petro-fabrics and seismic properties of blueschist and eclogite in the north Qilian suture zone, NW China: implications for the low-velocity upper layer in subducting slab, trench-parallel seismic anisotropy and eclogite detectability in the subduction zone. J. Geophys. Res. 118, 3037–3058. http://dx.doi.org/10.1002/jgrb.50212.

Cao, Y., Jung, H., Song, S., 2014. Microstructures and petro-fabrics of lawsonite blueschist in the north Qilian suture zone, NW China: implications for seismic anisotropy of subducting oceanic crust. Tectonophysics 628, 140–157. http://dx.doi.org/10.1016/j.tecto.2014.04.028.

Cao, Y., Jung, H., Song, S., Park, M., Jung, S., Lee, J., 2015. Plastic deformation and seismic properties in fore-arc mantles: a petrofabric analysis of the Yushigou Harzburgites, north Qilian suture zone, NW China. J. Petrol. 56, 1897–1944. http://dx.doi.org/10.1093./petrology/egv053.

Chantel, J., Mookherjee, M., Frost, D.J., 2012. The elasticity of lawsonite at high pressure and the origin of low velocity layers in subduction zones. Earth Planet. Sci. Lett. 349–350, 116–125. http://dx.doi.org/10.1016/j.epsl.2012.06.034.

Christensen, N.I., Mooney, W.D., 1995. Seismic velocity structure and composition of the continental crust: a global view. J. Geophys. Res. 100, 9761–9788. http://dx.doi.org/10.1029/95JB00259.

Davis, P.B., Whitney, D.L., 2006. Petrogenesis of lawsonite and epidote eclogite and blueschist, Sivrihisar Massif, Turkey. J. Metamorph. Geol. 24, 823–849. http://dx.doi.org/10.1111/j.1525-1314.2006.00671.x.

Dengo, G., 1985. Mid America: tectonic setting for the Pacific margin from Southern Mexico to North Western Colombia. In: Nairn, A.E.M., Stehli, F.G., Uyeda, S. (Eds.), The Ocean Basin and Margins. Plenum Press, New York, pp. 15–37.

Endo, S., Wallis, S.R., Tsuboi, M., Torres De León, R., Solari, L.A., 2012. Metamorphic evolution of lawsonite eclogites from the southern Motagua fault zone, Guatemala: insights from phase equilibria and Raman spectroscopy. J. Metamorph. Geol. 30, 143–164. http://dx.doi.org/10.1111/j.1525-1314.2011.00960.x.

Faccenda, M., Capitanio, F.A., 2013. Seismic anisotropy around subduction zones: insights from three-dimensional modeling of upper mantle deformation and SKS splitting calculations. Geochem. Geophys. Geosyst. 14, 243–262. http://dx.doi.org/10.1002/ggge.20055.

Faccenda, M., Burlini, L., Gerya, T.V., Mainprice, D., 2008. Fault-induced seismic anisotropy by hydration in subducting oceanic plates. Nature 455, 1097–1100. http://dx.doi.org/10.1038/nature07376.

Fountain, D.M., Boundy, T.M., Austrheim, H., Rey, P., 1994. Eclogite-facies shear zones—deep crustal reflectors? Tectonophysics 232 (441–424, doi:10.1016/0040-1951(94)90100-7).

Fujimoto, Y., Kono, Y., Hirajima, T., Kanagawa, K., Ishikawa, M., Arima, M., 2010. P-wave velocity and anisotropy of lawsonite and epidote blueschists: constraints on water transportation along subducting oceanic crust. Phys. Earth Planet. Inter. 183, 219–228. http://dx.doi.org/10.1016/j.pepi.2010.09.003.

Hacker, B.R., Abers, G.A., 2004. Subduction factory 3: an excel worksheet and macro for calculating the densities, seismic wave speeds, and H_2O contents of minerals and rocks at pressure and temperature. Geochem. Geophys. Geosyst. 5, Q01005. http://dx.doi.org/10.1029/2003GC000614.

Harlow, G.E., Hemming, S., Avé Lallemant, H., Sisson, V.B., Sorensen, S.S., 2004. Two high-pressure-low-temperature serpentinite-matrix mélange belts, Motagua fault zone, Guatemala: a record of Aptian and Maastrichtian collisions. Geology 32, 17–20. http://dx.doi.org/10.1130/G19990.1.

Healy, D., Reddy, S.M., Timms, N.E., Gray, E., Brovarone, A.V., 2009. Trench-parallel fast axes of seismic anisotropy due to fluid-dilled cracks in subducting slabs. Earth Planet. Sci. Lett. 283, 75–86. http://dx.doi.org/10.1016/j.epsl.2009.03.037.

Ji, S., Saruwatari, K., Mainprice, D., Wirth, R., Xu, Z., Xia, B., 2003. Microstructures, petrofabrics and seismic properties of ultra high-pressure eclogites from Sulu region, China: implications for rheology of subducted continental crust and origin of mantle reflections. Tectonophysics 370, 49–76. http://dx.doi.org/10.1016/S0040-1951(03)00177-X.

Katayama, I., Karato, S.-I., 2006. Effect of temperature on the B- to C-type olivine fabric transition and implication for flow pattern in the subduction zone. Phys. Earth Planet. Inter. 157, 33–45. http://dx.doi.org/10.1016/j.pepi.2006.03.005.

Katayama, I., Hirauchi, K., Michibayashi, K., Ando, J., 2009. Trench-parallel anisotropy produced by serpentine deformation in the hydrated mantle wedge. Nature 461, 1114–1117. http://dx.doi.org/10.1038/nature08513.

Kern, H., Gao, S., Jin, Z., Popp, T., Jin, S., 1999. Petrophysical studies on rocks from the Dabie ultrahigh-pressure (UHP) metamorphic belt, Central China: implications for the composition and delamination of the lower crust. Tectonophysics 301, 191–215. http://dx.doi.org/10.1016/S0040-1951(98)00268-6.

Kim, D., Katayama, I., Michibayashi, K., Tsujimori, T., 2013a. Rheological contrast between glaucophane and lawsonite in naturally deformed blueschist from Diablo range. Calif. Isl. Arc 22, 63–73. http://dx.doi.org/10.1111/iar.12003.

Kim, D., Katayama, I., Michibayashi, K., Tsujimori, T., 2013b. Deformation fabrics of natural blueschists and implications for seismic anisotropy in subducting oceanic crust. Phys. Earth Planet. Inter. 444, 8–21. http://dx.doi.org/10.1016/j.pepi.2013.06.011.

Kim, D., Katayama, I., Wallis, S., Michibayashi, K., Miyake, A., Seto, Y., Azuma, S., 2015. Deformation microstructures of glaucophane and lawsonite in experimentally deformed blueschists: implications for intermediate-depth intraplate earthquakes. J. Geophys. Res. 120, 1229–1242. http://dx.doi.org/10.1002/2014JB011528.

Mainprice, D., 1990. An efficient Fortran program to calculate seismic anisotropy from the lattice preferred orientation of minerals. Comput. Geosci. 16, 385–393. http://dx.doi.org/10.1016/0098-3004(90)90072-2.

Mainprice, D., Ildefonse, B., 2009. Seismic anisotropy of subduction zone minerals—contribution of hydrous phases. In: Lallemand, S., Funiciello, F. (Eds.), Front. Earth Sci.: Subduction Zone Geodynamics. Springer, pp. 63–84 http://dx.doi.org/10.1007/978-3-540-87974-9.

Mainprice, D., Silver, P.G., 1993. Interpretation of SKS-waves using samples from the subcontinental lithosphere. Phys. Earth Planet. Inter. 78, 257–280. http://dx.doi.org/10.1016/0031-9201(93)90160-B.

Mainprice, D., Barruol, G., Ben IsmaÏl, W., 2000. The anisotropy of the Earth's mantle: from single crystal to polycrystal. In: Karato, S., Forte, A.M., Liebermann, R.C., Masters, G., Stixrude, L. (Eds.), Mineral Physics and Seismic Tomography: From Atomic to Global. Geoph. Monog. Vol. 117, pp. 237–264.

Marroni, M., Pandolfi, L., Principi, G., Malasoma, A., Meneghini, F., 2009. Deformation history of the eclogite- and jadeite-bearing mélange from north Motagua fault zone, Guatemala: insights in the processes of a fossil subduction channel. Geol. J. 44, 167–190. http://dx.doi.org/10.1002/gj.1145.

Morales, L.F.G., Tommasi, A., 2011. Composition, textures, seismic and thermal anisotropies of xenoliths from a thin and hot lithospheric mantle (Summit Lake, southern Canadian Cordillera). Tectonophysics 507, 1–15. http://dx.doi.org/10.1016/j.tecto.2011.04.014.

Nakajima, J., Hasegawa, A., 2004. Shear-wave polarization anisotropy and subduction induced flow in the mantle wedge of Northeastern Japan. Earth Planet. Sci. Lett. 225, 365–377. http://dx.doi.org/10.1016/j.epsl.2004.06.011.

Okamoto, K., Maruyama, S., 1999. The high-pressure synthesis of lawsonite in the MORB + H_2O system. Am. Mineral. 84, 362–373.

Okay, A.I., 1980. Mineralogy, petrology, and phase relations of glaucophane-lawsonite zone blueschists from the Tavsanli region, Northwest Turkey. Contrib. Mineral. Petrol. 72, 243–255. http://dx.doi.org/10.1007/BF00376143.

Ono, S., 1998. Stability limits of hydrous minerals in sediment and mid-ocean ridge basalt compositions: implications for water transport in subduction zones. J. Geophys. Res. 103, 18253–18267. http://dx.doi.org/10.1029/98JB01351.

Ortega-Gutiérrez, F., Solari, L.A., Ortega-Obregón, C., Elías-Herrera, M., Martens, U., Morán-Icál, S., Chiquín, M., Keppy, J.D., Torres de León, R., Schaaf, P., 2007. The Maya–Chortís boundary: a tectonostratigraphic approach. Int. Geol. Rev. 49, 996–1024. http://dx.doi.org/10.2747/0020-6814.49.11.996.

Precigout, J., Almqvist, B.S.G., 2014. The Ronda peridotite (Spain): a natural template for seismic anisotropy in subduction wedges. Geophys. Res. Lett. 41, 8752–8758. http://dx.doi.org/10.1002/2014GL062547.

Prior, D.J., Boyle, A.P., Brenker, F., Cheadle, M.C., Day, A., Lopez, G., Peruzzo, L., Potts, G.J., Reddy, S., Spiess, R., Timms, N.E., Trimby, P., Wheeler, J., Zetterstrom, L., 1999. The application of electron backscatter diffraction and orientation contrast imaging in the SEM to textural problems in rocks. Am. Mineral. 84, 1741–1759.

Randle, V., 1992. Microtexture Determination and Its Applications. The Institute of Materials, Minerals and Mining, London, p. 174.

Randle, V., Engler, O., 2000. Introduction to Texture Analysis: Macrotexture, Microtexture and Orientation Mapping. CRC Press, London, p. 408.

Ratschbacher, L., Franz, L., Min, M., et al., 2009. The North American–Caribbean plate boundary in Mexico–Guatemala–Honduras. In: James, K.H., Lorente, M.A., Pindell, J.L. (Eds.), The Origin and Evolution of the Caribbean Plate. Geol. Soc. Lond. Spec. Publ. Vol. 328, pp. 219–293. http://dx.doi.org/10.1144/SP328.11.

Reynard, B., Bass, J.D., 2014. Elasticity of lawsonite and seismological signature of metamorphism and water cycling in the subducting oceanic crust. J. Metamorph. Geol. 32, 479–487. http://dx.doi.org/10.1111/jmg.12072.

Satsukawa, T., Michibayashi, K., Anthony, E.Y., Stern, R.J., Gao, S.S., Liu, K.H., 2011. Seismic anisotropy of the uppermost mantle beneath the Rio Grande rift: evidence from Kilbourne hole peridotite xenoliths, New Mexico. Earth Planet. Sci. Lett. 311, 172–181. http://dx.doi.org/10.1016/j.epsl.2011.09.013.

Schmidt, M.W., Poli, S., 1994. The stability of lawsonite and zoisite at high pressures: experiments in CASH to 92 kbar and implications for the presence of hydrous phases in subducted lithosphere. Earth Planet. Sci. Lett. 124, 105–118. http://dx.doi.org/10.1016/0012-821X(94)00080-8.

Schmidt, M.W., Poli, S., 1998. Experimentally based water budgets for dehydrating slab and consequences for arc magma generation. Earth Planet. Sci. Lett. 163, 361–379. http://dx.doi.org/10.1016/S0012-821X(98)00142-3.

Sinogeikin, S.V., Schilling, F.R., Bass, J.D., 2000. Single crystal elasticity of lawsonite. Am. Mineral. 85, 1834–1837.

Teyssier, C., Whitney, D.L., Toraman, E., Seaton, N.C.A., 2010. Lawsonite vorticity and subduction kinematics. Geology 38, 1123–1126. http://dx.doi.org/10.1130/G31409.1.

Tsujimori, T., Liou, J.G., Coleman, R.G., 2005. Coexisting retrograde jadeite and omphacite in a jadeite-bearing eclogite from the Motagua fault zone, Guatemala. Am. Mineral. 90, 836–842.

Tsujimori, T., Sisson, V.B., Liou, J.G., Harlow, G.E., Sorensen, S.S., 2006. Petrologic characterization of Guatemalan lawsonite eclogite: eclogitization of subducted oceanic crust in a cold subduction zone. In: Hacker, B.H., McClelland, W.C., Liou, J.G. (Eds.), Ultrahigh-Pressure Metamorphism: Deep Continental Subduction. Geol. Soc. Am. S. Vol. 403, pp. 147–168. http://dx.doi.org/10.1130/2006.2403(09).

van Keken, P.E., Hacker, B.R., Syracuse, E.M., Abers, G.A., 2011. Subduction factory: 4. Depth-dependent flux of H_2O from subducting slabs worldwide. J. Geophys. Res. 116, B01401. http://dx.doi.org/10.1029/2010JB007922.

Vitale Brovarone, A., Beyssac, O., 2014. Lawsonite metasomatism: a new route for water to the deep earth, earth planet. Sci. Lett. 393, 275–284. http://dx.doi.org/10.1016/j.epsl.2014.03.001.

White, R.S., McKenzie, D., O'Nions, R.K., 1992. Oceanic crustal thickness from seismic measurements and rare earth element inversions. J. Geophys. Res. 97, 19683–19715. http://dx.doi.org/10.1029/92JB01749.

Whitney, D.L., Evans, B.W., 2010. Abbreviations for names of rock-forming minerals. Am. Mineral. 95, 185–187. http://dx.doi.org/10.2138/am.2010.3371.

Worthington, J.R., Hacker, B.R., Zandt, G., 2013. Distingushing eclogite from peridotite: EBSD-based calculations of seismic velocities. Geophys. J. Int. 193, 489–505. http://dx.doi.org/10.1093/gji/ggt004.

Zhang, J., Green, H.W., 2007. On the deformation of UHP eclogite: from laboratory to nature. Int. Geol. Rev. 49, 487–503. http://dx.doi.org/10.2747/0020-6814.49.6.487.